

Synthetic Wearable Kidney: The Creation of a Thin-Film Nano Fibrous Composite Membrane for Blood Filtration

Dr. Michael Rothwell^{1*} and Dr. Alejandro Cruz²

^{1*}Senior Researcher, Department of Materials Science and Metallurgy, University of Cambridge, UK.

²Professor, Department of Materials Science and Metallurgy, University of Cambridge, UK.

Abstract--- The Synthetic Wearable Kidney (SWK), a remarkable medical innovation of the last century, has preserved many lives afflicted with advanced renal failure. The configurations of SWK have undergone significant evolution throughout years of exploration. The future trajectory of SWK is focused on downsizing, enhanced biological compatibility, and providing metabolic activities. A hollow-fiber membrane with precisely regulated blood and dialyses flow emerged as the predominant design of the contemporary SWK. Despite their proven efficacy in extending patient longevity, contemporary blood purifying systems remain flawed. The existing blood purification therapy is deficient in enhancing the patient's well-being, managing problems, and restoring metabolic processes. This paper presents a straightforward approach for the lightweight construction of a SWK utilizing an innovative dialysis/adsorption dual-purpose Thin-film Nano-Fibrous Composite (TNC) Membrane for Blood Filtration (BF). TNC membrane comprises a Polyvinyl Alcohol (PA) water-based gel as the separating stage and a nano-fibrous (NF) membrane integrated with Carboxyl Functionalized Zirconium-based Metal-Organic Framework (CF-ZR-MOF), designed to decrease the quantity of creatinine during dialysis and provide effective BF. Results illustrate that the filtration capacity of both CF-ZR-MOF and PA-TNC escalates with increasing quantity, with CF-ZR-MOF NP exhibiting a markedly superior capacity (about 78 mg/g) in contrast to PA-TNC (around 43 mg/g) at elevated quantities. Consequently, incorporating a separation feature in the TNC dialysis substrate may promote the creation of a compact SWK.

Keywords--- Synthetic Wearable Kidney, Thin-film, Nano-Fibrous Composite, Polyvinyl Alcohol, Dialysis, Blood Filtration.

Received: 14 - 10 - 2024; Revised: 20 - 11 - 2024; Accepted: 16 - 12 - 2024; Published: 30 - 01 - 2025

I. Overview of Artificial Kidney

The kidney is a complicated abdominal organ comprising about 20 specially designed cells (Borges & Schor, 2018). Injury to the kidneys results in conditions exhibiting both acute and long-lasting renal symptoms. An abrupt elevation in serum creatinine levels, often associated with a reduction in urine output, constitutes a specific type of acute renal failure (ARF). ARF signifies a range of pathological alterations, including cell death and necrosis of kidney cells, modifications in the absorption barrier, impaired renal filtration, the contraction of arteries, tubular blockage, and interstitial edema (Nourie et al., 2024). Conversely, in persistent kidney failure, impaired renal cells are not substituted with functioning tubular cells, resulting in cirrhosis and tubulointerstitial inflammation.

Renal transplantation is regarded as an efficacious intervention for chronic renal failure. This technique has global issues and constraints. The obstacles include insufficient organ donors, safety concerns (organ transplantation denial and infection), exorbitant transplant prices, inequitable resource allocation, and age-related factors and complications (Du et al., 2023). To provide an appropriate treatment strategy, it is essential to understand the anatomy and functioning components of the kidney. The left kidney is positioned significantly higher than the right kidney due to its closeness to the spleen. These two essential organs significantly contribute to the maintenance of bodily equilibrium. Each kidney is encased in a robust fibrous membrane that safeguards it.

The kidney's operational component, or tissue, is categorized into two primary sections: the outer layer and the membrane of the kidney (Ni et al., 2024). The renal cortex's outer layer is the kidney's external region, housing the glomeruli, the early segment of the nephrons, and the more distal tangled tubules. The medulla is

partitioned into renal edifice with their apex directed towards the renal pelvis. It is a cavity that gathers urine generated by the nephrons and channels it to the ureter. The nephron is the functioning component of the kidney (Nagendra et al., 2023).

The synthetic kidney, or dialyzer, is an important component of contemporary renal substitute treatment. In earlier times, advanced renal disease resulted in the cessation of an individual's life without BF and kidney transplantation. The dialysis technique has been established for years, starting at the beginning of the 20th century (Kumaran & Hanukoglu, 2020). Following the functional utilization of dialysis treatments, synthetic kidneys advanced swiftly. An improved dialyzer capable of enduring elevated pressures across the membrane facilitated unnecessary fluid elimination; a plate-style dialyzer reduced blood circulation resistance and enabled more precise ultra filtering; the reduction of erythromycin as a blood thinner for dialysis; and a sophisticated shunt for consistent blood vessel evaluation all advanced the evolution of kidney transplantation.

In 1960, the initial chronic dialysis center was founded in Seattle, rendering advanced renal illness no longer terminal (Kurkus & Ostrowski, 2019). Currently, BF is a conventional therapy globally for multitudes of patients suffering from conditions ranging from severe kidney damage to advanced renal disease. The healthcare sector continues to develop innovative dialyzers to enhance patient outcomes.

II. Materials and Methods

Synthesis of UiO-66-(COOH)₂ Nano Particles (NP)

The manufacture of UiO-66-(COOH)₂ NP, a zirconium-based MOF with carboxyl functional groups, often uses a solvothermal approach (Ding et al., 2021). A zirconium precursor, such as zirconium chloride (ZrCl₄), is first in a high-boiling-point solvent, such as dimethylformamide (DMF). The organic linkage H₄-benzene tetracarboxylic acid (H₄BTC) imparts carboxyl functionality and is concurrently dissolved in the same solvent. The two solutions are amalgamated to create a uniform reaction mixture, and an additive such as acetic acid may be included to regulate nucleation and particle size, enhancing the crystallinity of the MOF.

The mixture is then placed in a Teflon-lined autoclave and heated to 120°C –150°C for 12–24 hours to promote the coordination of zirconium ions with the carboxylic groups of the linker, resulting in the formation of the UiO-66 framework. Upon cooling, the product is isolated using centrifugation or filtering and washed many times with DMF and ethanol to eliminate residual precursors and contaminants. To improve porosity, the NP may be activated by immersion in ethanol and then subjected to vacuum drying at 100–120°C. The synthesis of UiO-66-(COOH)₂ entails critical processes, including the coordination of Zr⁴⁺ ions with the carboxylic groups of H₄BTC, the deprotonation of the linker, and regulated crystallization under solvothermal conditions.

Preparation of PA-TNC Membrane

The PA-TNC membrane was synthesized using the coating-reaction process described in prior publications (Zhu et al., 2019). Initially, 0.25 g of PA was combined with 10.1 g of distilled water and agitated for 5 hours at 75 °C to create a 2.5 wt% PA water-based solution. To enhance the mechanical characteristics and flatness of the surface of the NF film for easier coating, it was subjected to cold pressing at 7 MPa for one minute. Following rapid saturation with a 0.75 M boric acid solution, the pressurized NF film was affixed to a smooth, transparent plate using adhesive tape. The pH of the PA water-based solution was then adjusted to 3 via meticulous dropwise incorporation of 2 M hydrochloric acid. The resulting solution was combined with a certain quantity of Glutaraldehyde to initiate the binding process. The binding duration of the blended solution was observed before the initiation of the covering procedure.

The pre-binding liquid was ultimately deposited to the NF substrate using an automated film dispenser at the optimal pre-binding duration of 25 minutes and a temperature of 27 °C, preventing the solution from entering the surface. Furthermore, the PA-TNC membrane was fabricated via a coating process, with NF film as the base layer.

Creatinine Filtration Test

The filtration efficacy of UiO-66-(COOH)₂ NP and NF membrane on creatinine filtration was examined comprehensively. To establish the state of equilibrium of creatinine on CF-ZR-MOF NP and NF membrane, 12 mg of every NP and layer was immersed in 12 mL of a water-based creatinine liquid contained in a 25 mL specimen at 25 °C. The setup was secured to a shaker operating at 100 rpm for 24 hours to achieve adsorption equilibrium.

Initially, creatinine levels ranged from 150 to 850 mg/L. Following adsorption, the quantity of the remaining creatinine solution after the NP or film expulsion was quantified using an ultraviolet spectrophotometer and estimated based on established curves. The variation in the creatinine level between the dissolved solution and the initial mixture may validate the quantities of deposited creatinine. The absorption capacity, denoted as Q (mg/g), was contingent upon equation (1):

$$Q = (L_0 - L_e) * \left(\frac{V}{W}\right) \quad (1)$$

L_0 denoted the starting levels of creatinine (mg/L), whereas L_e indicated the optimal level of creatinine (mg/L). V (L) represented the quantity of the creatinine, whereas M (g) denoted the weight of the adsorbent used in the mixture.

Synthetic Wearable Kidney

Among all forms of renal replacement, a kidney transplant provides the highest quality of life, lowest overall financial expenditures, and superior success rate (Johansen et al., 2021). Nevertheless, the availability of transplanted kidneys is far lower than what is needed. Consequently, the majority of patients with advanced renal illness need BF or dialysis through the peritoneum for survival. The SWK is a desirable but formidable concept that arose with advancements in renal replacement treatment. The SWK must possess many characteristics to be implanted and effectively substitute the functions of human kidneys.

The power supply need must be minimized. A study involving pigs demonstrated that the silicon NP membrane's efficacy enables dialysis without pumping mechanisms for blood segments. The flow of blood constitutes one of the most enduring energy sources in the human body. If SWK relies on a battery for power, the battery must operate for many years to prevent the need for repeated surgical replacements.

Secondly, hemofiltration should be the preferred method of replacing the kidneys instead of BF. The SWK might be developed without pumping mechanisms for dialyses, eliminating the need for dialysate requirements. The need for a continuous supply of dialysate, an embedded input for dialyses, and substantial quantities of fresh water will cease, enabling the development of SWK. The gadget must have exceptional biocompatibility. The replacement treatment with SWK is conducted continuously throughout the day after transplantation. Coagulation and activated complement will be more pronounced than in standard discontinuous dialysis. An ongoing administration of heparin is also difficult. The NF membrane must be modified to avert such reactions unequivocally. NF membranes with super-non-fouling characteristics are viable options.

The metabolic capabilities of native kidney cells have long been overlooked in kidney transplant treatment—the absence of metabolic activity results in several complications in individuals with advanced renal illness. Bioreactors containing renal cells safeguarded by nanostructured elements have been developed for SWK. Furthermore, the superior defense against immune systems obviates the need for immune suppressant medications.

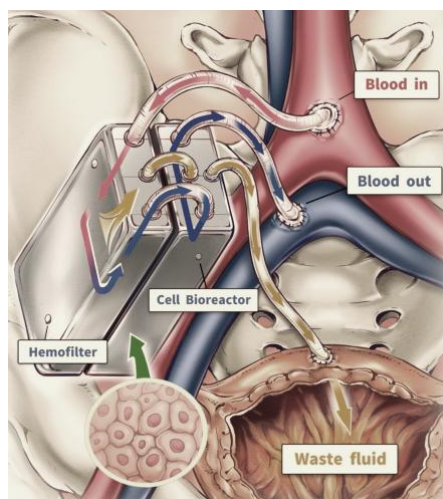


Figure 1: Synthetic Wearable Kidney

SWK might be produced with these four characteristics. The prosthetic kidney comprises a biological reactor and a hemofilter linked to the blood flow via the standard femoral vein and artery (Figure 1). The unwanted fluid is excreted into the individual's bladder as urine. The mechanism of hemofiltration relies on the tension differential between the arteries and veins. Post-implantation, patients might hypothetically sustain life without further dialysis.

III. Results and Discussion

Field Emission Scanning Electron Microscopy (FE-SEM) is an advanced technology extensively used for high-resolution visualization and characterization of surface topography and structural attributes of nano-materials.

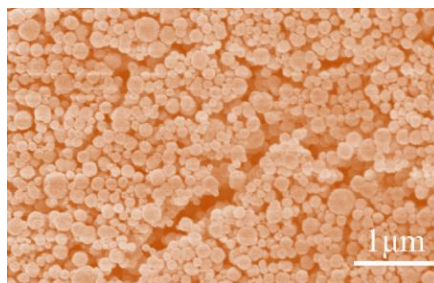


Figure 2: FE-SEM Image and the Variation in the Particle Size of the Synthesized CF-ZR-MOF NP

Figure 2 shows the typical FE-SEM image and the variation in the particle size of the synthesized CF-ZR-MOF NP, which exhibited a spherical morphology with an unrefined surface. The microscopic particles were non-uniform in size, with a mean diameter of 162 nm. It is important to highlight that the absence of CF-ZR-MOF NP aggregation rendered them ideal for electrically spinning in conjunction with a polymer matrix.

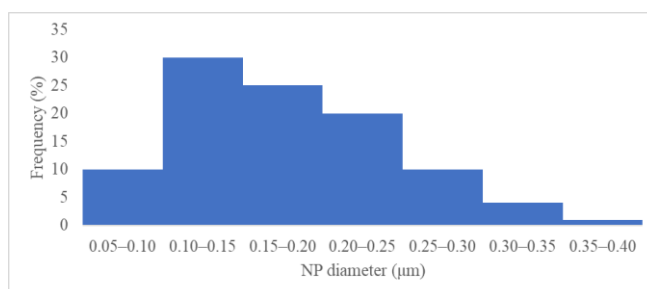


Figure 3: Distribution of CF-ZR-MOF NP Sizes According to their Frequency Percentages

Figure 3 depicts the distribution of CF-ZR-MOF NP sizes according to their frequency percentages. The predominant particle size range is 0.10–0.15 μm, comprising 30% of the overall distribution, followed by the 0.15–0.20 μm range at 25%. This signifies that smaller particles predominate the sample. The frequencies diminish progressively with increasing particle sizes, with the ranges of 0.20–0.25 μm and 0.25–0.30 μm accounting for 20% and 10%, respectively. The infrequent sizes fall between 0.30–0.35 μm and 0.35–0.40 μm, accounting for just 4% and 1%, respectively. This tendency indicates a biased distribution preferring smaller particle sizes, essential for applications dependent on tiny particle homogeneity and consistency.

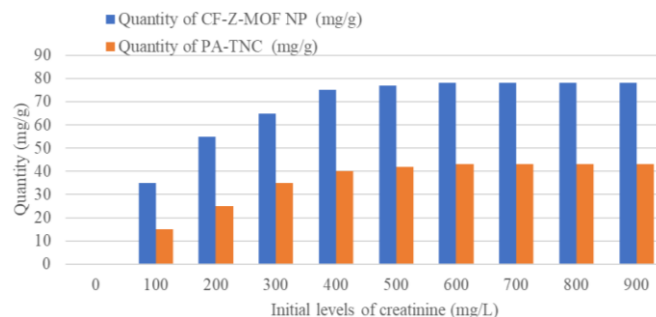


Figure 4: Quantity (mg/g) Versus Initial Creatinine Levels (mg/L) for CF-ZR-MOF NP and PA-TNC
<https://doi.org/10.67013/EPFS/V3I1/EPFS25101>

Figure 4 depicts the Quantity (mg/g) versus initial creatinine levels (mg/L) for CF-ZR-MOF NP and PA-TNC. Figure 4 clearly illustrates that the filtration capacity of both materials escalates with increasing quantity, with CF-ZR-MOF NP exhibiting a markedly superior capacity (about 78 mg/g) in contrast to PA-TNC (around 43 mg/g) at elevated quantities. This suggests that CF-ZR-MOF NP has enhanced adsorption characteristics, probably attributable to its greater surface area and functional groups.

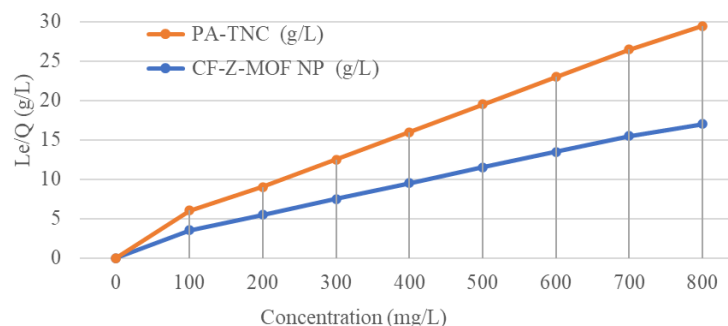


Figure 5: Concentration (mg/L) Versus Le/Q (g/L) for PA-TNC and CF-ZR-MOF NP

Figure 5 illustrates the Langmuir isotherm relationship, which indicates that the Le/Q values for CF-ZR-MOF NP are consistently greater than those for PA-TNC at all equilibrium creatinine concentrations. This further demonstrates that UiO-66-(COOH)₂ has a greater affinity and adsorption efficiency, making it a better choice for applications that need efficient adsorption at different concentrations.

Consequently, implementing a dialysis/adsorption dual-functioning TNC film would significantly reduce the dialysate required, presenting promising applications in SWK technology. Furthermore, asserting that the compact model remains relevant to other toxins beyond creatinine is plausible. Future studies will focus on developing novel adsorbent particles with enhanced toxin adsorption capability and accelerated adsorption rates for various toxins. The superior novel adsorbent compound will extract contaminants from the dialysate. They may also be integrated with the advanced TNC film to do compact BF more efficiently. This will also initiate a fresh investigation into the advancement of SWK technology.

IV. Conclusion

This work introduces a simple method for the lightweight fabrication of a SWK using a new dialysis/adsorption dual-purpose TNC Membrane for BF. The TNC membrane consists of a PA water-based gel as the separation layer and an NF membrane integrated with CF-ZR-MOF to reduce creatinine levels during dialysis and enhance blood filtration efficiency. The results demonstrate that the filtering capacity of both CF-ZR-MOF and PA-TNC increases with the amount, with CF-ZR-MOF NP showing a significantly higher capacity (about 78 mg/g) compared to PA-TNC (around 43 mg/g) at higher numbers. The Le/Q ratios for CF-ZR-MOF NP consistently exceed those of PA-TNC across all equilibrium creatinine concentrations. This further illustrates that UiO-66-(COOH)₂ has superior affinity and adsorption effectiveness, making it a more suitable option for applications requiring effective adsorption across varying concentrations.

References

- [1] Borges, F. T., & Schor, N. (2018). Regenerative medicine in kidney disease: where we stand and where to go. *Pediatric Nephrology*, 33, 1457-1465. <https://doi.org/10.1007/s00467-017-3754-9>
- [2] Nourie, N., Ghaleb, R., Lefaucheur, C., & Louis, K. (2024). Toward precision medicine: Exploring the landscape of biomarkers in acute kidney injury. *Biomolecules*, 14(1), 82. <https://doi.org/10.3390/biom14010082>
- [3] Du, Y., Shang, Y., Qian, Y., Guo, Y., Chen, S., Lin, X., ... & Zhang, Y. (2023). Plk1 promotes renal tubulointerstitial fibrosis by targeting autophagy/lysosome axis. *Cell Death & Disease*, 14(8), 571. <https://doi.org/10.1038/s41419-023-06093-4>
- [4] Ni, W. J., Li, Z. L., Wen, X. L., Ji, J. L., Liu, H., Yin, Q., ... & Wang, B. (2024). HIF-1 α and adaptor protein LIM and senescent cell antigen-like domains protein 1 axis promotes tubulointerstitial fibrosis by interacting with vimentin in angiotensin II-induced hypertension. *British Journal of Pharmacology*. <https://doi.org/10.1111/bph.16358>

- [5] Nagendra, L., Fernandez, C. J., & Pappachan, J. M. (2023). Simultaneous pancreas-kidney transplantation for end-stage renal failure in type 1 diabetes mellitus: Current perspectives. *World Journal of Transplantation*, 13(5), 208. <https://doi.org/10.5500/wjt.v13.i5.208>
- [6] Kumaran, G. K., & Hanukoglu, I. (2020). Identification and classification of epithelial cells in nephron segments by actin cytoskeleton patterns. *The FEBS journal*, 287(6), 1176-1194. <https://doi.org/10.1111/febs.15088>
- [7] Kurkus, J., & Ostrowski, J. (2019). Nils Alwall and his artificial kidneys: Seventieth anniversary of the start of serial production. *Artificial Organs*, 43(8). <https://doi.org/10.1111/aor.13545>
- [8] Ding, S., Zhang, T., Li, P., & Wang, X. (2021). Dialysis/adsorption bifunctional thin-film nanofibrous composite membrane for creatinine clearance in portable artificial kidney. *Journal of Membrane Science*, 636, 119550. <https://doi.org/10.1016/j.memsci.2021.119550>
- [9] Zhu, Y., Yu, X., Zhang, T., Hua, W., & Wang, X. (2019). Nanofibrous composite hemodiafiltration membrane: a facile approach towards tuning the barrier layer for enhanced performance. *Applied Surface Science*, 465, 950-963. <https://doi.org/10.1016/j.apsusc.2018.09.201>
- [10] Johansen, K. L., Chertow, G. M., Foley, R. N., Gilbertson, D. T., Herzog, C. A., Ishani, A., ... & Wetmore, J. B. (2021). US renal data system 2020 annual data report: epidemiology of kidney disease in the United States. *American journal of kidney diseases*, 77(4), A7-A8. <https://doi.org/10.1053/j.ajkd.2021.01.002>